# Effect of alloying on the electronic structure in CeNiSn

A. Ślebarski
*Institute of Physics, University of Silesia, 40-007 Katowice, Poland*

A. Jezierski
*Institute of Molecular Physics, Polish Academy of Sciences, 60-179 Poznań, Poland*

A. Zygmunt
*Institute for Low Temperature and Structure Research, Polish Academy of Sciences, 50-950 Wrocław, Poland*

S. Mähl, M. Neumann, and G. Borstel
*Universität Osnabrück, Fachbereich Physik, 49069 Osnabrück, Germany*

(Received 24 May 1996; revised manuscript received 22 July 1996)

The electronic structure of $CeNi_{1-x}Cu_xSn$ system and $Ce_{0.9}Zr_{0.1}NiSn$ is studied by photoemission spectroscopy. CeNiSn is a rare example of a valence-fluctuating Ce compound with a small gap at the Fermi energy. The gap is strongly suppressed by substituting either Cu for Ni or Zr for Ce. The XPS valence-band spectra are compared with *ab initio* band structure calculations, using the linearized muffin-tin orbital method. For CeNiSn a small indirect energy gap and a very low density of states at the Fermi level is found. The substitution of Ni by Cu leads to a higher density of states at Fermi energy, whereas for the substitution of Ce by even 10% Zr, the changes of the density of states at $\epsilon_F$ are clearly visible. A strong hybridization of the $f$ orbitals with a conduction band is characteristic for all of the investigated compounds. We report the Ce $3d$ XPS spectra of $CeNi_{1-x}Cu_xSn$ and $Ce_{0.9}Zr_{0.1}NiSn$. Applying the Gunnarsson-Schönhammer model the coupling energy $\Delta$ between the $f$ levels and the conduction states is about 115 meV. The number of $4f$ electrons $n_f$ is 0.95 for CeNiSn. With increasing Cu concentration, $n_f$ is close to 1. The magnetic susceptibility of $CeNi_{1-x}Cu_xSn$ and $Ce_{0.9}Zr_{0.1}NiSn$ is measured in magnetic fields from 50 Oe up to 5 T. [S0163-1829(96)05343-X]

## I. INTRODUCTION

Cerium-base Kondo-lattice systems exhibit interesting physical phenomena such as valence fluctuations and heavy-fermion behavior.[1,2] The low-temperature properties of the latter are dominated by a renormalized narrow band formed by the hybridization and a Kondo-type interaction between the $4f$ electron and the conduction electrons. Most Kondo-lattice systems have a metallic ground state, either magnetically ordered or Pauli paramagnetic.

The class of Ce compounds with unstable $4f$ shells was recently enlarged by a new group of intermetallics with nonmetallic behavior at low temperatures. The well known semiconducting compounds such as SmS, SmSe, $SmB_6$, or $YbB_{12}$ are based on the rare-earth elements with the $4f$ shells nearly half-filled or nearly filled. CeNiSn (Refs. 3 and 4) is the first example of a valence-fluctuating cerium compound with an energy gap which is an order of magnitude smaller than those in the above mentioned compounds. To the group of these new systems belong the compounds $Ce_3Bi_4Pt_3$ (Ref. 5) and CeRhSb.[6] At low temperatures these ternary intermetallics show a characteristic semiconducting behavior which is believed to arise from hybridization between $4f$ and conduction-band electrons. Transport properties of these materials show Kondo behavior at high temperatures and formation of a gap at low temperatures.

The gap in CeNiSn is unstable against any change in $4f$-conduction electron hybridization caused by alloying[7,8] and application of pressure[9] or magnetic field.[10] Alloying studies of CeNiSn revealed that the gap is closed by any replacement of about 10% either of the Ni sublattice or Ce sublattice. Magnetic, thermal, and transport measurements on $CeNi_{1-x}Cu_xSn$ have demonstrated the evolution from a valence-fluctuating state with an energy gap to an antiferromagnetic Kondo state for $x>0.13$ through a heavy-fermion state.[7] In Ref. 11 the authors compare the resistivities of several single crystals of CeNiSn and suggest a semimetallic ground state of a clean sample, while impurer ones are semiconductors. This is the case where an increase in purity changes a semiconductor to a metallic conductor; usually it is in the other way around.

In order to elucidate the mechanism of gap formation we measured the structural and magnetic properties and the electronic structure of ternary $CeNi_{1-x}Cu_xSn$ compounds. The valence-band XPS spectra are compared with calculations of the electronic structure of the valence bands by the self-consistent spin-polarized linear-muffin-tin orbital (LMTO) method. In this work we present the electronic structure calculations of CeNiSn, where Ni or Ce is substituted by different $d$ elements. The calculations show the destructive influence of the substituted element either in the Ni or Ce atomic positions on the gap formation at the Fermi energy. We also

 

TABLE I. The lattice parameters $a$, $b$, and $c$ in Å.

| | | | |
|---|---|---|---|
| CeNiSn | 7.544 | 4.601 | 7.619 |
| $Ce_{0.9}Zr_{0.1}NiSn$ | 7.552 | 4.601 | 7.634 |
| $CeNi_{0.98}Cu_{0.02}Sn$ | 7.5455 | 4.601 | 7.625 |
| $CeNi_{0.95}Cu_{0.05}Sn$ | 7.560 | 4.608 | 7.634 |
| $CeNi_{0.9}Cu_{0.1}Sn$ | 7.575 | 4.613 | 7.652 |
| $CeNi_{0.7}Cu_{0.3}Sn$ | 7.477 | 4.6275 | 7.635 |
| CeCuSn (hexag.) | 4.593 | 4.593 | 7.882 |

note that the calculated densities of states at $\epsilon_F$ are relatively small in the $CeNi_{1-x}Cu_xSn$ system, even for CeCuSn, which does not show any gap at the Fermi energy.

## II. EXPERIMENT

The samples $CeNi_{1-x}Cu_xSn$ were arc melted of the constituent metals on a cooled copper crucible in a high-purity argon atmosphere, remelted several times, and then homogenized at 800 °C for 1 week. The compounds were identified by their powder diagrams, which were recorded in x-ray Debye-Scherer powder diffraction with Cu$K_\alpha$ radiation using the Siemens D-5000 diffractometer. The crystal parameters are given in Table I.

A SQUID magnetometer and vibrating magnetometer were used to obtain the magnetization results at low temperatures from 1.6 up to 300 K and magnetic fields of 50 Oe to 50 kOe.

The XPS spectra of $CeNi_{1-x}Cu_xSn$ were obtained with monochromatized Al $K\alpha$ radiation at room temperature using a PHI 5600ci ESCA spectrometer. The energy spectra of the electrons were analyzed by a hemispherical mirror analyzer with an energy resolution of 0.4 eV. All spectra were measured in vacuum below $6\times10^{-10}$ Torr. Calibration of the spectra was performed according to Ref. 12. Binding energies were referenced to the Fermi level ($\epsilon_F=0$), the $4f$ levels of gold were found at 84.0 eV, and the observed energy spread of electrons detected at Fermi energy was about 0.4 eV. In all the compounds investigated we have detected in the XPS spectra a small amount of oxygen, which comes mainly from the impurity phase $Ce_2O_3$. This phase was also detected by others[11] in several single crystals of CeNiSn, which were grown by different methods.

The electronic structure of the ordered CeNiSn (orthorhombic space group *Pnma*), CeCuSn (hexagonal space group $P6_3mmc$) and $CeNi_{1-x}Cu_xSn$ alloys was studied by the self-consistent tight binding linearized muffin-tin orbital (TB LMTO) method[13,14] within the atomic sphere approximation (ASA) and the local spin density (LSD) approximation. The exchange correlation potential was assumed in the

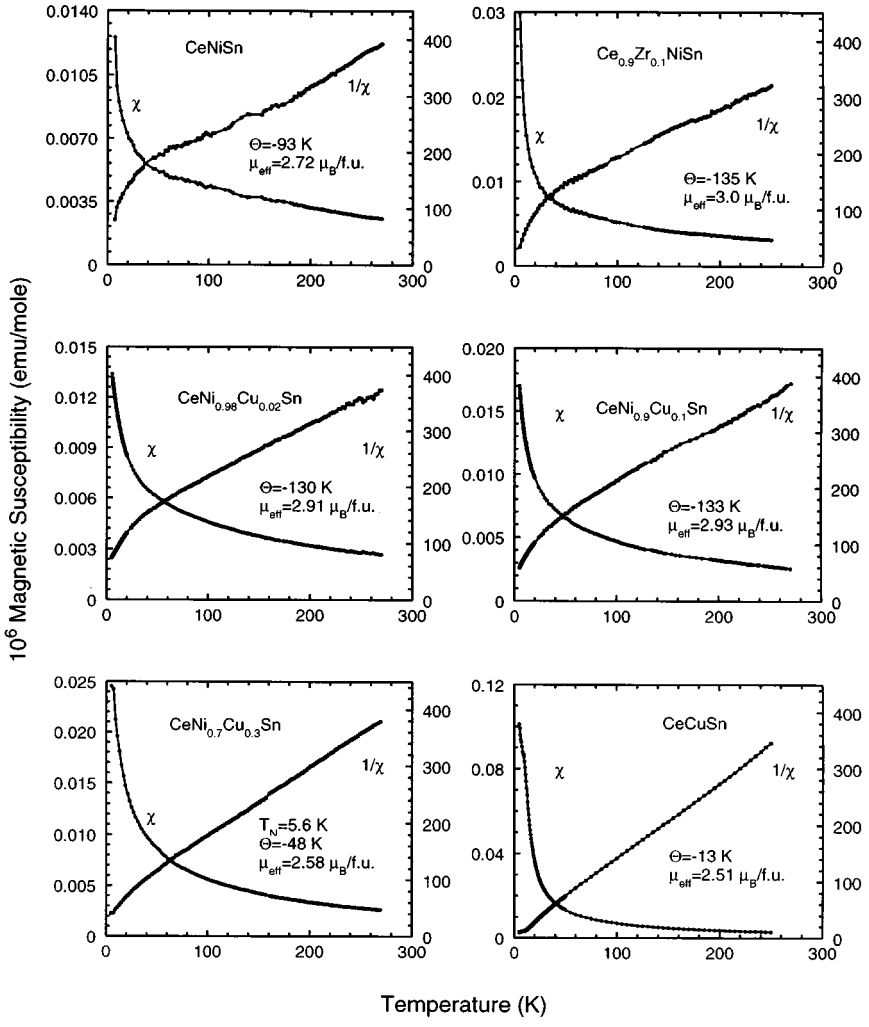


FIG. 1. Magnetic susceptibility $\chi$ in emu/mole and the inverse susceptibility $1/\chi$ in mole/cm$^3$ as a function of temperature for CeNiSn, $Ce_{0.9}Zr_{0.1}NiSn$, $CeNi_{0.98}Cu_{0.02}Sn$, $CeNi_{0.9}Cu_{0.1}Sn$, $CeNi_{0.7}Cu_{0.3}Sn$, and CeCuSn. The applied magnetic field is 10 kOe.

form proposed by von Barth-Hedin,[15] and Langreth-Mehl-Hu (LMH) corrections[16] were included. In the band calculations we assumed the initial configurations according to the Periodic Table of elements. The electronic structures were computed for the experimental lattice parameters. The spin-orbit coupling was included for the valence electrons.[17] The band structures for $CeNi_{1-x}Cu_xSn$ alloys were calculated for the supercell $Ce_8Ni_{8-y}Cu_ySn$, where for $y$ we put 1 and 2. The number of $k$ points in the irreducible part of the Brillouin zone was 216 for the orthorhombic structure, 193 for the hexagonal structure, and 64 for the $Ce_8Ni_{8-y}Cu_ySn$ supercell. For calculations of the electronic structure of $Ce_{0.85}Zr_{0.15}NiSn$ we used a supercell with 32 atoms and for closed packing four empty spheres were considered.

## III. RESULTS AND DISCUSSION

### A. Magnetic properties of $CeNi_{1-x}Cu_xSn$

The magnetic properties of CeNiSn are discussed, e.g., in Ref. 4. We have analyzed in details the susceptibility of the $CeNi_{1-x}Cu_xSn$ system at different magnetic fields (50 Oe $< H <$ 50 kOe) as a function of temperature. The main goal of these systematic investigations was to find out the influence of the impurities on these anomalous Ce materials. The impurity phase $Ce_2O_3$ was always found, even in very good quality single crystals, by electron-probe microanalysis[11] or specific heat measurements.[18] Most of the published magnetic investigations of CeNiSn are carried out at strong magnetic fields of the order of several kOe. We analyzed the system at a very weak magnetic field, at which the presence of additional phases of $Ce_2O_3$ is less than 0.02%. For small $x$ the low temperature magnetization is also dominated by the impurity, which contributes to a Brillouin term, taking into account a mean-field approximation for the magnetic ordering. Figure 1 presents the susceptibility and inverse susceptibility of six $CeNi_{1-x}Cu_xSn$ alloys. At liquid helium temperatures the impurity phase gives the main contribution to the susceptibility. Above $T=150$ K the susceptibility is determined by the bulk material. The influence of the gap on the susceptibility of CeNiSn is not evident in this experiment, however the alloying changes the magnetic properties of the system. When Ni is substituted by Cu, the concentration of $d$-type electrons increases in the band. As a consequence one expects a change of the magnetic properties in relation to CeNiSn, caused by the change of hybridization between $f$ and conduction-band states. Indeed, the slope of the magnetization plotted as a function of the magnetic field ($H$) increases systematically with $x$ (see Fig. 2). Moreover, the magnetization $\mu$ vs $H$ deviates from linearity when $x$ is small, and even for $x = 0.05$ the $\mu(H)$ dependence is characteristic for the metamagnetic phase transition (Fig. 2). Ce substituted by tetravalent Zr changes the distribution mainly of the $d$ states in the band; however, we do not observe a change of the magnetic properties with respect to CeNiSn. For the concentration of Cu larger than 20% the susceptibility follows the Curie-Weiss law and indicates an antiferromagnetic ordering (Figs. 1 and 2).

Figure 2 shows the magnetization of CeCuSn at $T=4.2$ K as a function of the magnetic field. The singularities observed at the critical fields, $H_{c1}=15$ kOe, and $H_{c2}=26$ kOe are connected with the presence of magnetic transitions. The magnetization below $H_{c1}$ is linear with $H$ and typical for noncollinear antiferromagnetism, at $H_{c1}$ there is the transition to the second noncollinear antiferromagnetic phase and at $H_{c2}$ the metamagnetic-type transition to the ferromagnetic phase is observed. The destruction of the zero-field impurity phase is visible again. The value of $T_N$ is dependent on the applied magnetic field. Our results are in agreement with magnetic properties of CeCuSn proposed in Ref. 19. The inverse susceptibility as a function of temperature follows the Curie-Weiss law above $T=50$ K and gives $\mu_{\text{eff}}=2.51$ $\mu_B$/f.u. and $\Theta=-13$ K.

### B. Electronic properties of $CeNi_{1-x}Cu_xSn$

Figure 3 compares the XPS valence bands of $CeNi_{1-x}Cu_xSn$ and $Ce_{0.9}Zr_{0.1}NiSn$ intermetallics with the band of $CeNi_2Sn_2$. The XP valence-band spectra of $CeNi_2Sn_2$ and CeNiSn are similar, the 3$d$ Ni peaks are located 1 eV below the Fermi energy, and we conclude that those states are mostly occupied. The 3$d$ Cu states are located at about 3.5 eV below $\epsilon_F$. The energetic distributions of these states are rather broad when the Cu concentration is smaller than 10%, however for the $x=0.3$ compound and CeCuSn the 3$d$ Cu peak is more localized and more narrow.

At a binding energy of about 10 eV the satellite structure in the XP valence-band spectra is observed. The XP valence-band spectra are compared with the results of our calculations of the electronic structure of CeNiSn and $CeNi_{1-x}Cu_xSn$. In Fig. 4 we present the plots of the total

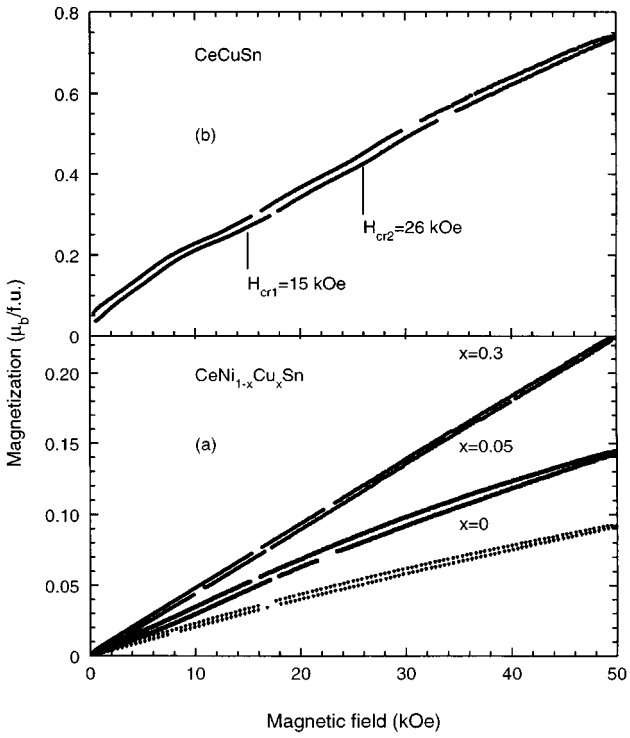


FIG. 2. Magnetization as a function of magnetic field at $T=4.2$ K for $CeNi_{1-x}Cu_xSn$ (a) and for CeCuSn (b).

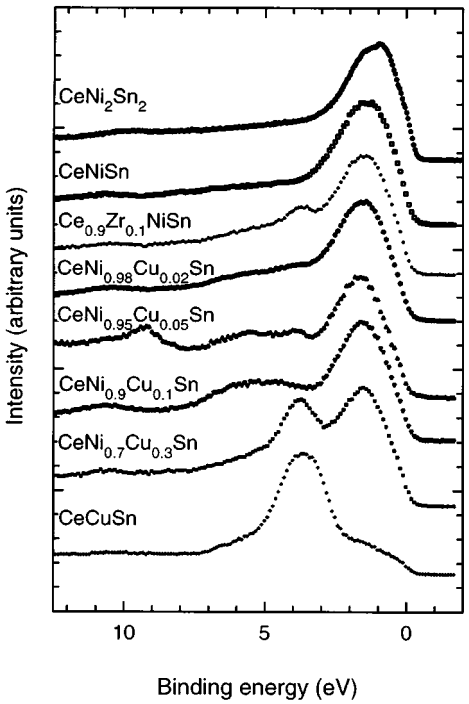


FIG. 3. The valence band XPS spectra for $CeNi_{1-x}Cu_xSn$ and $Ce_{0.9}Zr_{0.1}NiSn$ compared with the spectrum for $CeNi_2Sn_2$.

density of states for CeNiSn, $CeNi_{0.85}Cu_{0.15}Sn$, $Ce_{0.875}Zr_{0.125}NiSn$, and CeCuSn, and the Fermi level is located at $E=0$ eV.

Figure 5 presents the DOS of Ce, Cu, Ni, and Sn for $CeNi_{0.75}Cu_{0.25}Sn$. Now we can analyze the shape of the

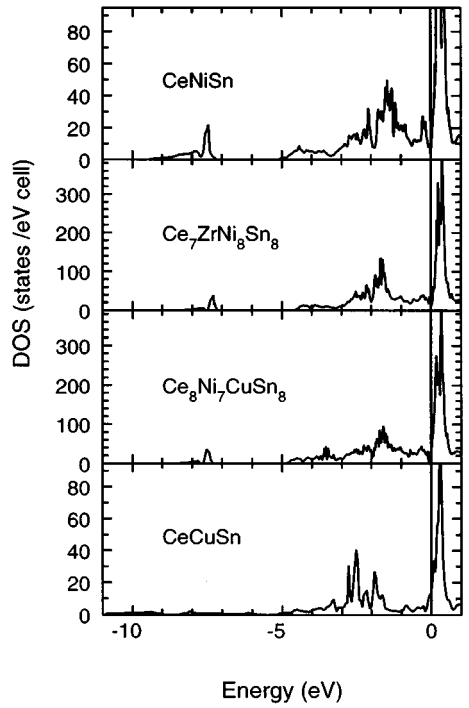


FIG. 4. Calculated total densities of states (DOS) for CeNiSn, $Ce_{0.85}Zr_{0.15}NiSn$, $CeNi_{0.85}Cu_{0.15}Sn$, and CeCuSn. The position of the Fermi energy is at $E=0$ eV.

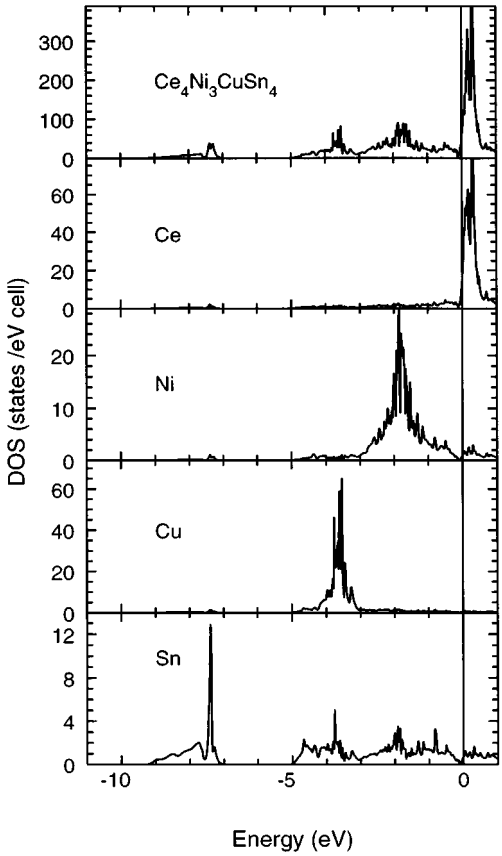


FIG. 5. Total and partial densities of states for $CeNi_{0.75}Cu_{0.25}Sn$. The energy scale is represented relative to the Fermi energy. Total DOS is presented in states/(eV cell), partial DOS in states/(eV atom).

XPS-VB intensity plots presented in Fig. 3. The narrow peaks located at about 3.5 eV are mainly connected with the 3*d* Cu states, but the ''satellite'' at 10 eV indicates the distribution of Sn 5*s* states. 4*f* Ce states are distributed at $\epsilon_F$ and below at the occupied side of the band. The broad peaks at about 5.5 eV could represent the distribution of the valence-band states of Sn; however, they are mostly due to some surface oxygen contamination.

The calculated value of DOS at $\epsilon_F$ is 0.07 for CeNiSn, 0.49 for $CeNi_{0.85}Cu_{0.15}Sn$, 0.74 for $CeNi_{0.75}Cu_{0.25}Sn$, and 1.19 (states/eV atom) for CeCuSn. When Ce atoms in CeNiSn are partly substituted by Zr, the calculated DOS at the Fermi energy slightly increases with respect to CeNiSn and equals $\sim 0.15$ (states/eV atom). The units [states/(eV atom)] used for the DOS are different from those of Figs. 4 and 5, but they are more representative for a comparison of the DOS at the Fermi energy of the alloys described by either orthorhombic (CeNiSn) or hexagonal (CeCuSn)-type structures and reflect the number of states per one atom in each unit cell. We observe a correlation between the lattice parameters and the electronic properties of $CeNi_{1-x}Cu_xSn$ alloys. The calculated densities of states (DOS) at the Fermi energy $\epsilon_F$ are not linear with $x$, but show a similar tendency to the volume, when plotted as function of the Cu concentration.

Figure 6 presents the band structure of CeNiSn and of CeCuSn plotted along various symmetry directions. CeNiSn

TABLE II. 3*d* XPS peak binding energies for Ce intermetallic compounds (all values in eV with respect to $\varepsilon_F$).

| Compound | $3d_{5/2}$ | $3d_{3/2}$ |
|---|---|---|
| $CeNi_2Sn_2$ | 885.38 | 903.88 |
| CeNiSn | 885.15 | 903.61 |
| $Ce_{0.9}Zr_{0.1}NiSn$ | 885.17 | 903.70 |
| $CeNi_{0.98}Cu_{0.02}Sn$ | 885.29 | 903.81 |
| $CeNi_{0.95}Cu_{0.05}Sn$ | 885.29 | 903.81 |
| $CeNi_{0.9}Cu_{0.1}Sn$ | 885.40 | 903.81 |
| $CeNi_{0.7}Cu_{0.3}Sn$ | 885.29 | 903.70 |
| CeCuSn | 885.29 | 903.58 |

is a semimetal, with an indirect gap. The bands cross the Fermi level only in $\Gamma - X$ and $\Gamma - Y$ directions. Our calculated electron bands are very close to those obtained by Yanase and Harima,[20] who used the LAPW method with the local density approximation. For the other compounds of the $CeNi_{1-x}Cu_xSn$-type we observe some $k$ directions for which the calculated bands do not cross the Fermi energy, but the densities of states at $\varepsilon_F$ are much larger than for CeNiSn.

The subband of states below $\sim 2$ eV in respect to $\epsilon_F$ consists of strongly hybridized Ce 5*d*, Ni 3*d*, and Sn 5*p* states. It is possible to estimate the hybridization $\Delta$ of *f* electrons with the conduction states from the relative intensities of the Ce 3*d* XPS peaks (see Table II). $\Delta$ is defined as $\pi V^2 \rho_{\max}$, where $\rho_{\max}$ is the maximum in density of conduction states and $V$ is the hybridization matrix element. Figure 7 illustrates the Ce 3*d* XPS spectra of $CeNi_{1-x}Cu_xSn$. The spin-orbit splitting dominates the spectral structure of the 3*d* XPS peaks of Ce intermetallics. At the low-binding-energy side of the $3d_{5/2}$ and $3d_{3/2}$ lines the shake down satellites are observed, which are known to account for the screened Ce $3d^9 4f^1$ final states.[21–23] The shift of the shake down satellites in relation to the main peak is about 4 eV. The creation of the core hole pushes an empty 4*f* level below the Fermi energy. The Coulomb interaction between the core hole and 4*f* states pushes an empty 4*f* level below the Fermi energy. A conduction electron fills the hole with a probability proportional to the hybridization energy $\Delta$.[23] The 3*d* spin-orbit-split components show in the Ce XPS spectrum additional structures at higher energy with an energy separation of order 13 eV with respect to the main peak.

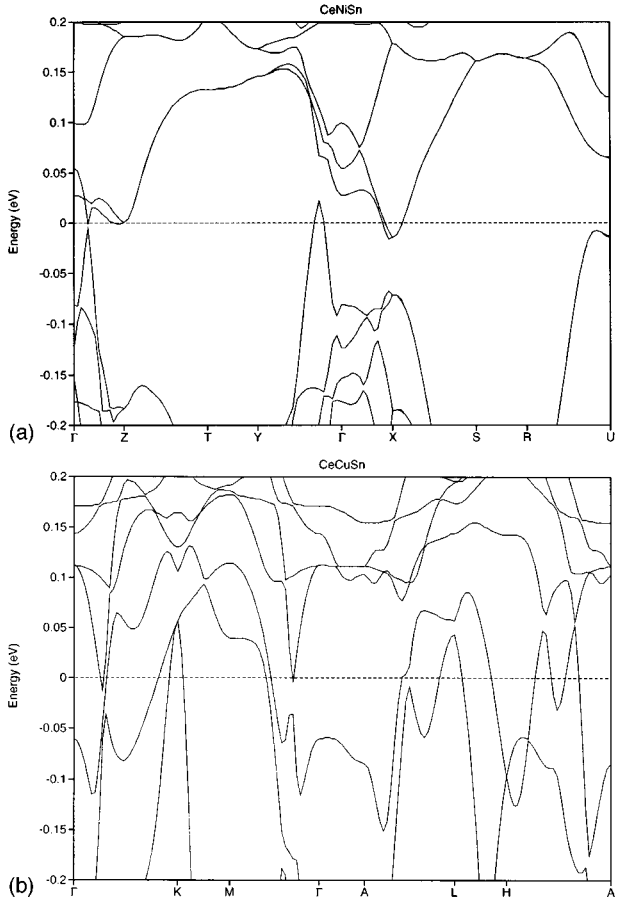


FIG. 6. The band structure of CeNiSn and CeCuSn calculated near the Fermi energy along various symmetry directions.

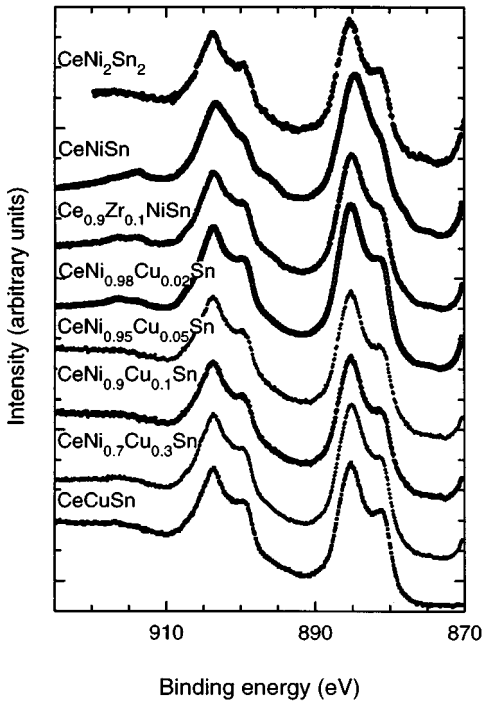


FIG. 7. The Ce 3*d* XPS spectra obtained with the monochromatized Al K$\alpha$ radiation.

The structure in the Ce 3*d* XPS spectra is interpreted in terms of the Gunnarsson-Schönhammer theory.[24] Gunnarsson and Schönhammer, using a slightly modified version of the Anderson impurity Hamiltonian, calculated XPS Ce spectra and discussed how experimental spectra can be used to estimate the $f$ occupancy, $n_f$, and the coupling $\Delta$.

When the intensities of the final $3d^9f^1$ and $3d^9f^2$ states are measured, it is possible to determine the coupling $\Delta$ from the ratio $r=I(f^2)/I(f^1)+I(f^2)$ calculated in Ref. 25 as a function of $\Delta$. The hybridization width for $\alpha$-Ce estimated in this way is $\Delta=60$ meV.[26] For Ce intermetallic compounds with strong $f$ shell instabilities $\Delta$ is about 150 meV.[25] The separation of the peaks of Ce 3*d* XPS spectra (Fig. 7) that overlap was made on the base of the Doniach-Sunjić theory.[27] For CeNiSn the intensity ratio $r=0.24$ was obtained with an accuracy of 5%. This value of $r$ gives from the calculated variation of $r$ as a function of $\Delta$ (Ref. 25) hybridization width $\Delta\approx 115$ meV. The coupling $\Delta$ is quite large, larger than that obtained for $\alpha$-Ce (Ref. 26) but smaller than that for $CeNi_2Sn_2$.[28] We measured in the same way the hybridization width $\Delta$ for $CeNi_{1-x}Cu_xSn$ and $Ce_{0.9}Zr_{0.1}NiSn$, which in these cases is comparable with $\Delta$ of CeNiSn. We suggest that the gap-formation in Kondo insulators depends on the hybridization strength, but first of all on the energy of the subbands location in respect to $\epsilon_F$. Alloying shifts the hybridization process to higher energy in relation to $\epsilon_F$ in the $CeNi_{1-x}Cu_xSn$.

CeNiSn has proven to be a rare example of a valence-fluctuating Ce compound with an energy gap. The high energy component of $3d_{3/2}$ and $3d_{5/2}$ multiplets can be interpreted as a contribution of the $4f^0$ configuration to the Ce ground state.[24] We have evaluated the intensity ratio $f^0/(f^0+f^1+f^2)$,[24,25] which should be directly related to the $f$ occupation in the final state. For CeNiSn XPS indicates an $f$ occupation $n_f\approx 0.95$. The $3d^9f^0$ component for 3*d* multiplets clearly is observed too for Ce substituted by tetravalent Zr and for 2% of Cu alloy. A shoulder in the high energy tail of the Ce 3*d* XPS spectrum at 913.3 eV is not due to the tail of the oxygen 1*s* Auger line. This high energy peak is detected too when the spectra are obtained with Mg K$\alpha$ radiation (Fig. 8). For comparison, $CeNi_2Sn_2$ with the stable trivalent Ce configuration $4f^15d^16s^2$ obtained by XPS (Ref. 28) and by $L_{III}$ x-ray absorption[29] measurements does not show the satellite at 913 eV (Fig. 8). This satellite is not clearly observed in the Ce 3*d* XPS spectra of $CeNi_{1-x}Cu_xSn$ when $x>0.02$. We conclude that the valence fluctuation properties of Ce in the CeNiSn Kondo insulator vanish when Ni is substituted by a second transition metal with deeper located *d* states in the band.

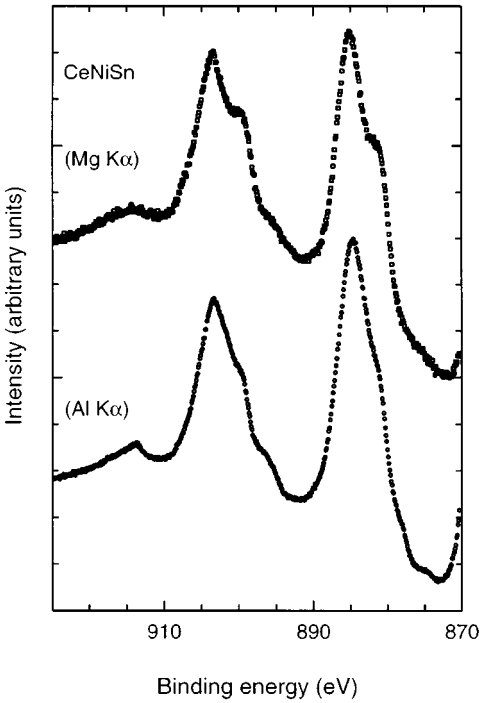


FIG. 8. The Ce 3*d* XPS spectra obtained for CeNiSn with the Mg K$\alpha$ and Al K$\alpha$ radiation.

The partial distributions of the electronic states suggest strong hybridization of the $f$-conduction electrons type. We observe the important influence of the energy location of *d* subbands of the substituted element on the gap formation. Tetravalent Zr does not show a maximum of the calculated DOS at about 3.5 eV below the Fermi energy, there is only a small amount. We suppose that Zr modifies the DOS of other components through the strong hybridization effect. The magnetic measurements found the presence of a Ce-impurity phase in CeNiSn and its alloys, less than 0.02%. Even a very careful technology is not able to remove the additional Ce phases in this compound.[11] When Ni is substituted by Cu, the concentration of *d* electrons in the band slightly increases and modifies the band structure. For example, the magnetization measured as a function of the magnetic field at $T=4.2$ K and at $H=50$ kOe increases with increasing Cu in $CeNi_{1-x}Cu_xSn$. The susceptibility of CeNiSn and its alloys is typical for the Kondo system with a bigger value of $\mu_{\text{eff}}$ than is expected for a $Ce^{3+}$ ion and quite a large Curie-Weiss constant without a presence of magnetic ordering.

## IV. CONCLUSIONS

The calculations of the electronic structure of CeNiSn-type compounds found an indirect energy-gap for CeNiSn, and substitution either on the Ni or on the Ce sublattice suppresses the gap. The density of states at the Fermi energy increases when Ni is substituted by Cu. The observed increment of DOS correlates with the lattice parameters and unit volume of $CeNi_{1-x}Cu_xSn$ system. There seems to be generally good agreement between the band structure (total DOS) calculations and the experimental XPS valence-band spectra.

## ACKNOWLEDGMENTS

This work was partly supported by the Foundation for Polish Science (Project SUBIN Nr 10/95), by the Deutscher Akademischer Austausch Dienst (DAAD), and by the Deutsche Forschungsgemeinschaft (DFG). One of us (A.J.) thanks the State Committee for Scientific Research for financial support (Project No. 2P30200507) and Dr. A. Postnikov for the discussion on the spin-orbit coupling contributions to the TB LMTO code. The calculations were made in the Supercomputing and Networking Centre of Poznań.

[1] Z. Fisk *et al.*, Science **239**, 225 (1989).
[2] N. Grewe and F. Steglich, in *Handbook on Physics and Chemistry of Rare Earth*, edited by K. A. Gschneidner, Jr. and L. Eyring (Elsevier Science Publishers B. V., Amsterdam, 1991), Vol. 14, p. 343.
[3] T. Takabatake, Y. Nakazawa, and M. Ishikawa, Jpn. J. Appl. Phys. **26**, 547 (1987).
[4] T. Takabatake *et al.*, Phys. Rev. B **41**, 9607 (1990).
[5] S. K. Malik and D. T. Androja, Phys. Rev. B **43**, 6277 (1991).
[6] M. F. Hundley *et al.*, Phys. Rev. B **42**, 6842 (1990).
[7] T. Takabatake *et al.*, J. Magn. Magn. Mater. **76/77**, 87 (1988).
[8] S. Nishigori *et al.*, Physica B **186/188**, 406 (1993).
[9] M. Kurisu, T. Takabatake, and H. Fujiwara, Solid State Commun. **68**, 595 (1988).
[10] T. Takabatake *et al.*, Physica B **199/200**, 457 (1994).
[11] G. Nakamoto *et al.*, J. Phys. Soc. Jpn. **64**, 4834 (1995).
[12] Y. Baer, G. Busch, and P. Cohn, Rev. Sci. Instrum. **46**, 466 (1975).
[13] O. K. Andersen, O. Jepsen, and M. Sob, in *Electronic Structure and Its Applications*, edited by M. Yussouff (Springer, Berlin, 1987), p. 2.
[14] O. K. Anderson, Tight-Binding LMTO ver. 4.7.
[15] U. von Barth and L. Hedin, J. Phys. C **5**, 1629 (1972).
[16] C. D. Hu and D. C. Langreth, Phys. Scr. **32**, 391 (1985).
[17] B. I. Min and Y.R. Jang, J. Phys. Condens. Matter **3**, 5131 (1991).
[18] S. Nishigori *et al.*, Physica B **199/200**, 473 (1994).
[19] H. Nakotte *et al.*, J. Alloys Compounds **207/208**, 245 (1994).
[20] A. Yanase and H. Harima, Prog. Theor. Phys. Suppl. **108**, 19 (1992).
[21] G. K. Wertheim, R. L. Cohen, A. Rosencweig, and H. J. Guggenheim, in *Electron Spectroscopy*, edited by D. A. Shirley (North-Holland, Amsterdam, 1972), p. 813.
[22] G. Crecelius, G. K. Wertheim, and D. N. E. Buchanan, Phys. Rev. B **18**, 6519 (1978).
[23] J. C. Fuggle *et al.*, Phys. Rev. Lett. **45**, 1597 (1980).
[24] O. Gunnarsson and K. Schönhammer, Phys. Rev. B **28**, 4315 (1983).
[25] J. C. Fuggle *et al.*, Phys. Rev. B **27**, 7330 (1983).
[26] E. Wuilloud, H. R. Moser, W. D. Schneider, and Y. Baer, Phys. Rev. B **28**, 7354 (1984).
[27] S. Doniach and M. Šunjić, J. Phys. C **3**, 285 (1970).
[28] A. Ślebarski *et al.* (unpublished).
[29] G. Liang, N. Jisravi, and M. Croft, Physica B **163**, 134 (1990).